Experimental Evidence for Supercontinuum Generation by Fission of Higher-Order Solitons in Photonic Fibers

J. Herrmann,[1,*] U. Griebner,[1] N. Zhavoronkov,[1] A. Husakou,[1] D. Nickel,[1] J. C. Knight,[2] W. J. Wadsworth,[2] P. St. J. Russell,[2] and G. Korn[1,†]

[1]*Max Born Institute for Nonlinear Optics and Short Pulse Spectroscopy, Max-Born-Strasse 2a, D-12489 Berlin, Germany*

[2]*Department of Physics, University of Bath, Claverton Down, Bath BA2 7AY, United Kingdom*

(Received 15 November 2001; published 11 April 2002)

We report on an experimental study of supercontinuum generation in photonic crystal fibers with low-intensity femtosecond pulses, which provides evidence for a novel spectral broadening mechanism. The observed results agree with our theoretical calculations carried out without making the slowly varying envelope approximation. Peculiarities of the measured spectra and their theoretical explanation demonstrate that the reason for the white-light generation in photonic crystal fibers is fission of higher-order solitons into redshifted fundamental solitons and blueshifted nonsolitonic radiation.

DOI: 10.1103/PhysRevLett.88.173901 PACS numbers: 42.70.Qs, 42.65.Re, 42.81.Dp

Photonic crystal fibers (PCFs) based on wavelength-scale microstructuring of fiber cladding are currently a topic of high interest because of their unusual optical properties and their large potential for important applications. In a typical realization [1,2] a PCF has a central region of pure silica (core) surrounded by air holes as seen in the cross section of the PCF in Fig. 1(a). Light is guided by total internal reflection as in standard step-index fibers due to the refractive index difference between the core and the holey cladding. The large difference of the indices for μm-diameter core provides a very strong specifically controlled waveguide contribution to dispersion which leads to significant modification in the optical properties such as single-mode operation over a wide range of wavelengths [2], a shift of zero-dispersion wavelength into the visible region [3,4], and soliton propagation at optical frequencies [4,5]. In a different realization light can also be guided in a hollow core of a PCF due to the photonic band gap of the periodic photonic crystal cladding [6].

As a result of the dispersion characteristics of PCFs, notable features in nonlinear optical effects arise that differ greatly from those in standard fibers at the same pulse parameters. One such phenomenon which has attracted considerable attention is the recently demonstrated generation of an extremely broadband supercontinuum (SC) covering more than two octaves from low-energy ($\sim$1 nJ) pulses with an initial duration $\tau_0 = 100$ fs [3]. The analogous effect has also been observed in tapered fibers made by heating and stretching a standard fiber to form a narrow thread of silica surrounded by air [7]. In comparison, SC generation in standard fibers requires more than 2 orders of magnitude higher initial peak intensities I_0 [8–10]. The dramatic spectral broadening of relatively low-intensity pulses in PCFs is an interesting phenomenon and has already been used in several fascinating applications. Significant progress in frequency metrology [11,12] has been achieved using the generation of an octave-spanning optical frequency "comb" in a PCF by a train of fs laser pulses. SC generated in a PCF is also an excellent source for optical coherence tomography with ultrahigh resolution in biological tissue [13]. Further there is a large potential for numerous applications such as for pulse compression, laser spectroscopy, all-optical telecommunication, dispersion measurements, sensor technique, and others.

Despite these important applications, the mechanism of low-intensity SC generation in PCFs was not understood up to a short time ago. In a recent theoretical Letter [14] it was shown that low-intensity SC generation in

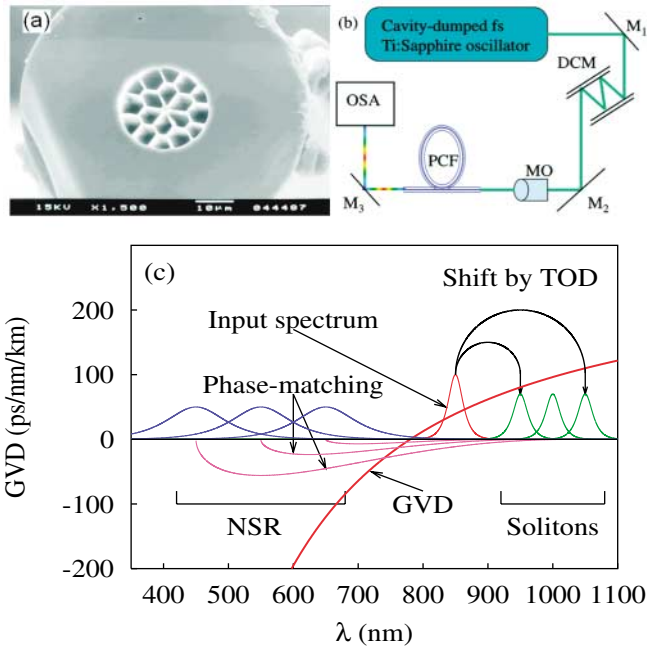

FIG. 1 (color). Cross section of the 2.5-μm PCF (a), experimental setup (b), and schematic of supercontinuum generation (c). $M_{1,2,3}$, mirrors; DCM, dispersion-precompensating chirped mirror pair; MO, the microscopic objective; OSA, the optical spectrum analyzer.

PCFs is caused not by self-phase modulation but by fission of higher-order solitons. In this Letter, we present the experimental evidence for this new mechanism for SC generation.

The formation of SC by the interaction of intense pulses with matter was discovered first in condensed matter [15] and later also in single-mode fibers (for an overview, see [16]). The physical origin of this effect is refractive index change by the electric field $\Delta n = n_2 I(t)$, where $I(t)$ is the intensity and n_2 is the nonlinear refractive index. As a result a time-dependent phase is induced which implies the generation of new spectral components around the input frequency ω_0 with maximum spectral width $\Delta\omega_{\mathrm{SPM}}/\omega_0 = 1.39 n_2 I_0 L/\tau_0 c$ [17], L being the propagation length. Normal group-velocity dispersion (GVD) limits this width while in the anomalous dispersion region the balance of GVD and self-phase modulation (SPM) leads to the formation of solitons. At higher amplitudes a higher-order soliton with soliton number N is formed. Such a bounded N soliton undergoes periodic narrowing and broadening without breakup during propagation, if higher-order effects can be neglected. However, for femtosecond higher-order solitons with a frequency near the zero-dispersion point third-order dispersion, the contribution from the Raman effect and the self-steepening effect play a important role. They lead to a breakup of N solitons into their constituent 1 solitons [18] and the emission of blueshifted nonsolitonic radiation (NSR) [19–22] (for an overview, see [17]).

The low-intensity spectral broadening observed in PCFs cannot be explained by the effect of SPM for low-energy pulses in the range of 1 nJ and 100 fs duration. With these parameters, the maximum spectral broadening by SPM is $\Delta\omega_{\mathrm{SPM}}/\omega_0 \approx 0.07$, while the experiments yield $\Delta\omega_{\mathrm{SPM}}/\omega_0 \sim 1$. Recent theoretical work [14] has given a surprising explanation: SC generation by low-intensity pulses in the anomalous dispersion region is caused by fission of higher-order solitons into redshifted fundamental solitons. Because of third-order dispersion every emerging 1-soliton emits blueshifted phase-matched NSR. Since all solitons and their corresponding NSR possess distinct central frequencies, the width of the generated spectrum increases with increasing soliton number or with pulse duration. In direct contrast to SPM, for which shorter pulses are more favorable, SC generation by fission of N solitons is more effective for long pulses, which can be used as a test for soliton-induced SC generation.

To study the physical mechanism for low-intensity SC generation in PCFs we have performed several experiments with different input and PCF parameters and compared the results of the measurements with theoretical simulations. In our experiments [see Fig. 1(b)] we used a cavity dumped beam from a Ti:sapphire oscillator with a pair of prisms incorporated for GVD control. To adjust the wavelength of radiation as well as its bandwidth a variable slit was introduced into the dispersive arm of the cavity. Almost transform-limited pulses centered at 850 or 807 nm with pulse durations of 29 and 100 fs for both wavelengths were generated. For these wavelengths the GVD is anomalous in our PCF. We can smoothly change the repetition rate keeping the pulse energy constant but decreasing the average power to prevent overheating of the fiber. The pulse energy could be changed quite easily by altering the rf power delivered to the dumper; also the laser is not sensitive to feedback from the fiber tip which could interrupt the mode locking in the case of an ordinary fs oscillator. To keep the pulses spectrally limited after passing through the focusing microscope objective a combination of fused-silica pair of prism and negative-GVD ($\sim$40 fs^2 per bounce) mirrors was used. The PCFs are air-silica 40-cm-long microstructured fibers with core diameters of $d = 1.6$ and 2.5 μm and zero-dispersion wavelengths of 670 and 790 nm, respectively. The spectra generated in the fibers covered the range up to 350–1600 nm and were measured with an optical spectrum analyzer (ANDO AQ-6315A). The peak intensity in the fundamental mode inside the fiber was estimated from the measured power behind the fiber. Part of the launched power was guided in cladding or higher-order modes and formed the undepleted fundamental peak. This fraction was determined from the experimental spectra [Figs. 2(a) and 2(b)] and accounted for the given intensities.

For the theoretical description of pulse propagation with a spectral width $\Delta\omega$ comparable with or even larger than the carrier frequency ω_0 standard approximations of nonlinear optics such as the slowly varying envelope approximation (SVEA) and a truncated Taylor expansion for the linear susceptibility cannot be used. With the neglect of backward reflection, a first-order wave equation can be derived [14] which is not limited to the range of small spectral bandwidths as the SVEA:

$$\frac{\partial \tilde{E}(z,\omega)}{\partial z} = i\left(\beta(\omega) - \frac{\omega}{c}\right)\tilde{E}(z,\omega) + i\,\frac{\mu_0\omega^2}{2\beta(\omega)}\,P_{NL}(z,\omega)\,. \tag{1}$$

Here $P_{NL}(z,\omega)$ is the Fourier transform of $P_{NL}(z,t) = \epsilon_0\chi_3\tilde{E}(z,t)^3$; the electric field in frequency domain is separated into $\mathbf{E}(x,y,z,\omega) = \mathbf{F}(x,y,\omega)\tilde{E}(z,\omega)$, where $\tilde{E}(z,\omega)$ is the longitudinal distribution. The contribution of the Raman effect is not significant for the parameters considered here, as checked by numerical calculation. Note that the Raman-induced frequency shift reported recently in Ref. [5] was observed for infrared input frequency for a lower relative third-order dispersion parameter. The transverse fundamental mode distribution $\mathbf{F}(x,y,\omega)$ is the solution of the Helmholtz equation for a PCF with the eigenvalue $\beta(\omega)$. To calculate $\beta(\omega)$ for the fundamental mode, we approximate the effective refractive index of the cladding $n_{\mathrm{eff}}(\omega)$ [2,14]

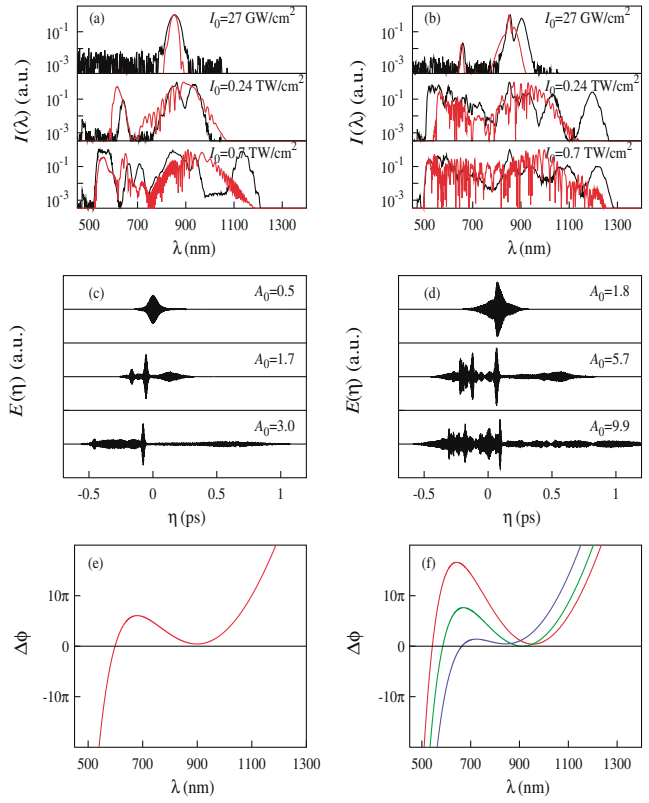

FIG. 2. Measured (black) and calculated (red) spectra (a),(b), pulse shapes (c),(d), and phase difference (e),(f) for $\tau_0 = 29$ fs (a),(c),(e) and $\tau_0 = 100$ fs (b),(d),(f) in a PCF with a 2.5-μm core diameter. Input wavelength is 850 nm.

with that of a photonic crystal using silica-air boundary conditions and periodicity conditions at the boundary of an elementary cell. In Fig. 2(a) the measured output spectra for a PCF with a core diameter of 2.5 μm is presented for a 29-fs input pulse with three different peak intensities 27 GW/cm^2, 0.24 TW/cm^2, and 0.7 TW/cm^2, centered at 850 nm, and in Fig. 2(b) the same is shown for a 100-fs pulse (black curves). Pulse energies are 0.024, 0.21, and 0.62 nJ, correspondingly. As can be seen, for an intensity of 0.24 TW/cm^2 [middle section of Fig. 2(a)] the spectrum of the 29-fs pulse is slightly broadened with an additional blueshifted side peak, while the 100-fs pulse generates a supercontinuum extending from 500–1300 nm. For 3 times higher intensity the spectral width of both pulses increases, but the spectrum of the longer pulse is flatter. The largest extension of the spectrum from 350 to 1600 nm we observed for an intensity 2.7 TW/cm^2 with the 100-fs pulse (not shown). As can be seen particularly by comparison of the middle section of Figs. 2(a) and 2(b), our observations are in direct contrast with the behavior of spectral broadening by SPM: a larger bandwidth is generated for a longer pulse with the same input intensity. To explain this phenomenon, we calculated the spectra [red curves in Fig. 2(a) and 2(b)] and temporal shapes [Fig. 2(c) and 2(d)] after propagation through the fiber by numerical integration of Eq. (1). Comparison of theoretical and experimental spectra reveals good agreement in width and characteristic features and allows one to identify the physical mechanism for SC in PCFs. Since the input frequency of the pulses in Fig. 2 is inside the anomalous dispersion region, a higher-order soliton is formed with the soliton number N which is the integer closest to $A_0 = \sqrt{n_2 I_0 (\tau_0/1.76)^2 \omega_0/\beta''(\omega_0)c}$; A_0 scales as the pulse duration. Because of the influence of third-order dispersion (TOD) the higher-order soliton splits into fundamental redshifted 1-solitons and loses energy by emitting blueshifted NSR [18–22] [see the scheme in Fig. 1(c)]. Because of the downshift of their central frequencies, the generated 1-solitons stabilize themselves after a certain propagation length. The pulse durations of the 1-solitons are determined approximately by $\tau_n = \tau_0/\xi_n$ [18] and their frequency shift by $\Delta\omega_s \approx 7/\tau_n$ [19], where $\xi_n = 2A_0 - n, n = 1, 2, \ldots, N$ are determined by the eigenvalues of the nonlinear Schrödinger equation. This scenario explains the observed and numerically calculated features in Fig. 2 and the given rough analytical estimates for τ_n and $\Delta\omega_s$ are supported by our numerical computations, with acceptable deviations. The input parameters in the middle section of Figs. 2(b), 2(d), and 2(f) imply the formation of an $N = 6$ soliton ($A_0 = 5.69$); the fission of this pulse into six short fundamental solitons can be seen in Fig. 2(d) together with a longer pulse which is the blueshifted NSR. As checked by numerical calculations, the separated short spikes are phase locked and satisfy the relation for a fundamental soliton $A_0 = 1$; their temporal shapes do not change over a distance of 7 cm while a linear pulse would drastically spread over this distance. The two shortest and most intense solitons have durations of 12 and 15 fs and redshifts of $-0.17\omega_0$ and $-0.09\omega_0$. The blueshifted part of the continuum in Fig. 2(b) arises as NSR emitted by and phase matched to the corresponding solitons. The phase of a soliton at frequency ω_s and that of the NSR are given by $\phi_s = \beta(\omega_s)L + n_2 I_0 \omega_s L/2c - \omega_s L/c$ and $\phi_r = \beta(\omega)L - \omega L/v_s$, respectively. In Fig. 2(f) the phase difference $\Delta\phi$ for the most intense soliton (red curve), the third strongest soliton (green curve), and the weakest soliton (blue curve) with respect to their NSR are presented; phase-matching $\Delta\phi = 0$ is realized for these solitons at 542, 586, and 664 nm, respectively. Thus every soliton emits radiation only at a certain frequency interval. Since the central frequencies of the solitons are different, distinct spectral fractions of NSR arise covering the range from 500 to 850 nm. In contrast the soliton number for the 28-fs pulse in the middle section of Figs. 2(a), 2(c), and 2(d) is $N = 2$ ($A_0 = 1.7$). Therefore, two solitons are formed [Fig. 2(c) middle]; one of them is weak, long, and its frequency shift is small. The stronger soliton with central wavelength 898 nm produces NSR only in a small isolated interval around 600 nm, as predicted

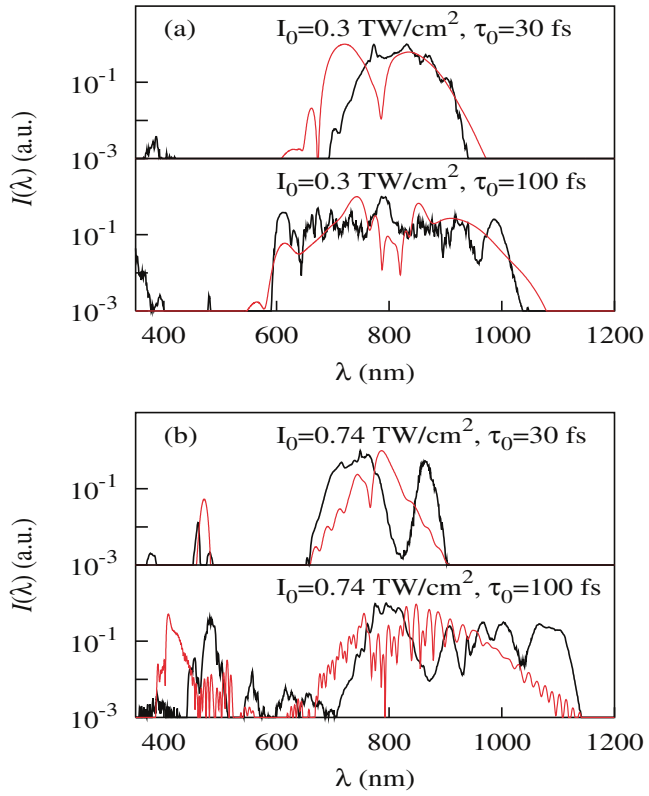

FIG. 3. Measured (black curves) and calculated (red curves) spectra for the 2.5-μm-diameter PCF (a) and the 1.6-μm-diameter PCF (b). Input wavelength is 807 nm.

by phase matching $\Delta\phi = 0$ in Fig. 2(e). This explains why the shorter 29-fs pulse with the same peak intensity yields a narrower spectrum in Fig. 2(a) than the longer 100-fs pulse. For the lower intensity, no solitons emerge ($A_0 = 0.5$) for the 29-fs input pulse, as can be seen in the top sections of Figs. 2(a) and 2(c), while for the 100-fs input pulse one redshifted soliton is formed [top section of Figs. 2(b) and 2(d)] together with blueshifted radiation. This radiation is seen as a small peak at ~650 nm in the top section of Fig. 2(b); the wavelength is in agreement with the numerical results (red curve). With increasing intensity in the bottom sections in Fig. 2 the short 29-fs pulse forms $N = 3$ solitons and can also generate a broad spectrum, but the spectrum of the 100-fs pulse with the same intensity is much smoother due to the fission into ~10 fundamental solitons. The fast oscillations in the numerically calculated spectrum arise due to the interference of the different solitons; in the measured spectra in Figs. 2(a) and 2(b) these oscillations cannot be observed, because resolution of the optical spectral analyzer was not sufficient for that. To study the crucial role of the dispersion characteristics we performed a number of additional experiments with a different input frequency and a different PCF. As an example, in Fig. 3(b) the measured and calculated spectra for a 30-fs and a 100-fs pulse are shown for a PCF with a diameter of 1.6 μm and a zero-dispersion point at 670 nm. The input wavelength at 805 nm is now deeper inside the anomalous region. We also studied propagation near the zero-dispersion point in the 2.5-μm PCF with the same input wavelength [Fig. 3(a)]. Again, in both cases we observe wider spectra for longer pulses in both theory and experiment.

In conclusion, we have provided the experimental evidence that low-intensity supercontinua in PCFs arise in the anomalous dispersion region through fission of higher-order solitons into redshifted fundamental solitons and blueshifted NSR is shown. This new mechanism for spectral broadening explains the peculiarities and the effectiveness of low-intensity SC generation in PCFs.

*Electronic address: jherrman@mbi-berlin.de
†Also at Katana Technologies GmbH, Albert-Einstein-Ring 7, 14532 Kleinmachnow, Germany.

[1] J. C. Knight *et al.,* Opt. Lett. **21**, 1547 (1996).
[2] T. A. Birks, J. C. Knight, and P. St. J. Russel, Opt. Lett. **22**, 961 (1997).
[3] J. K. Ranka, R. S. Windeler, and A. J. Steinz, Opt. Lett. **25**, 25 (2000).
[4] W. J. Wadsworth *et al.,* Electron. Lett. **36**, 53 (2000).
[5] X. Liu *et al.,* Opt. Lett. **26**, 358 (2001).
[6] J. C. Knight *et al.,* Science **282**, 1476 (1998).
[7] T. A. Birks, W. J. Wadsworth, and P. St. J. Russel, Opt. Lett. **25**, 1415 (2000).
[8] R. C. Fork *et al.,* Opt. Lett. **12**, 483 (1987).
[9] M. Pshenichnikov, W. de Boeij, and D. Wiersma, Opt. Lett. **19**, 572 (1994).
[10] V. P. Kalosha and J. Herrmann, Phys. Rev. A **62**, 011804 (2000).
[11] D. A. Jones *et al.,* Science **288**, 635 (2000).
[12] R. Holzwarth *et al.,* Phys. Rev. Lett. **85**, 2264 (2000).
[13] J. Hartl *et al.,* Opt. Lett. **26**, 608 (2001).
[14] A. V. Husakou and J. Herrmann, Phys. Rev. Lett. **87**, 203901 (2001).
[15] R. R. Alfano and S. L. Shapiro, Phys. Rev. Lett. **24**, 592 (1970).
[16] *The Supercontinuum Laser Source,* edited by R. Alfano (Springer-Verlag, New York, 1989).
[17] G. P. Agrawal, *Nonlinear Fiber Optics* (Academic Press, New York, 1994).
[18] Y. Kodama and A. Hasegawa, IEEE J. Quantum Electron. **23**, 510 (1987).
[19] P. K. A. Wai *et al.,* Opt. Lett. **12**, 628 (1987).
[20] N. Akhmediev and M. Karlsson, Phys. Rev. A **51**, 2602 (1995).
[21] J. N. Elgin, T. Brabec, and S. M. J. Kelly, Opt. Commun. **114**, 321 (1995).
[22] A. S. Gouveiv-Neto, M. E. Faldon, and R. J. Taylor, Opt. Lett. **13**, 1029 (1988).